Urban rainfall characteristics and permeable pavement structure optimization for sponge road in North China

Zhe Li, Yuanbo Cao, Jiupeng Zhang and Wolong Liu

ABSTRACT

Permeable asphalt pavement types are generally selected according to local traffic volume and rainfall intensity. This study focuses on the design of the pavement drainage asphalt pavement combination scheme by analyzing the rainfall characteristics of five representative cities in North China. Furthermore, nine kinds of drainage pavement scheme applicable to Beijing are proposed. To this end, the permeable function design analysis, as well as the bearing capacity design analysis of permeable asphalt pavement, was carried out with the help of storm runoff simulation software SWMM5.1 and pavement structure analysis software BISAR3.0, respectively. The results indicate that the minimum total design thickness of permeable surface layer and permeable basic layer meeting the requirements of road drainage in this region is 170 mm, and the nine drainage pavement schemes meet the specification requirements.

Key words | bearing capacity, drainage pavement, pavement engineering, permeable road, rainfall characteristics, sponge city

Zhe Li
Yuanbo Cao
Jiupeng Zhang (corresponding author)
Chang'an University,
Xian,
China
E-mail: zhjiupeng@chd.edu.cn

Wolong Liu
China Airport Construction Group Corporation,
Guangzhou,
China

HIGHLIGHTS

- Proposed nine combinations of different thicknesses of permeable pavements.
- Verified the feasibility of the nine combinations.
- Analyzed the intensity of rainstorm in five cities in North China.
- Comparison and selection of drainage pavement schemes.

INTRODUCTION

In recent years, with the acceleration of urbanization and the sharp increase of urban traffic, compacted cement concrete and dense-graded asphalt mixtures have become the first choice for pavement materials. Although such impermeable material is easy to construct, is low cost, and has good strength and durability, it will increase road noise and reduce rainfall infiltration into the ground. In addition, heavy rainfall will cause water on the road surface, thereby increasing the probability of traffic accidents. As an important part of a sponge city, permeable pavement has

excellent water permeability, drainage and noise reduction functions, and is gradually being used in newly built and rebuilt urban roads (Bean *et al.* 2019; Kia *et al.* 2019; Wendling & Holt 2019; Tziampou *et al.* 2020).

Based on so many advantages of drainage asphalt pavement, relevant scholars all over the world have carried out a lot of research on drainage asphalt pavement. Afonso and colleagues researched and developed a double-layer porous asphalt (DLPA) pavement drainage structure, and proved the effectiveness of DLPA to retain thick surface deposits and restrict fine particle deposits from entering the remaining layers (Afonso *et al.* 2017). Sun *et al.* (2019) researched the stress characteristics of unsaturated permeable asphalt pavement under load, and believed that the internal drainage of the pavement is crucial to the life

of the asphalt pavement. Manikanta and Reddy found that adding recron-ls fiber to permeable asphalt pavement can improve the performance of permeable asphalt pavement (Manikanta & Reddy 2018). Heweidak and Amin researched the hydraulic characteristics of OASIS phenolic foam material and applied it to permeable pavement to further estimate the optimal thickness of the OASIS layer required to delay peak rainwater flow under the maximum rainfall intensity (Heweidak & Amin 2019). Liu *et al.* (2018) researched a new type of evaporation-enhanced permeable pavement with better cooling and permeable effect. Whether it is simulated rainfall or real rainfall in Shanghai, China, this new type of pavement can increase water evaporation and improve road drainage effectively. Luo (2017) used finite element software ABAQUS to explore the stress characteristics of permeable asphalt pavement with an asphalt stabilized permeable base (ATPB) layer, and found that ATPB with good drainage can not only remove the water in the road structure and reduce road water damage effectively, but also reduce the stress concentration at the crack tip, which delays and inhibits the reflection of the semi-rigid substrate. Yin and co-workers found through indoor experiments that for the permeable asphalt pavement with a cement stabilized permeable base (CTPB) layer, when the optimal porosity of CTPB is set to 20%, it not only has good drainage capacity and absorption capacity for rainwater pollutant chemical oxygen demand, but also has greater strength, rigidity, better durability and resistance to water damage, and can be applied to places with high requirements for road bearing capacity (Yin *et al.* 2018). Masoud and colleagues evaluated the hydraulic performance of the permeable pavement of the highway and found that the porosity of the road surface and base needs to be carefully designed according to the specific situation (rather than the maximum possible permeability) to ensure the water permeability and structural bearing capacity (Masoud *et al.* 2019). In short, the current research on drainage asphalt pavement mainly focuses on drainage material composition and drainage structure design, but the biggest problem in the research process is that the road drainage performance and bearing capacity cannot be well balanced. Therefore, it has certain practical significance to study the drainage pavement structure design based on the two angles of drainage performance and road performance.

This paper mainly analyzes the chronological distribution characteristics and accumulated rainfall of the rainstorm intensity in North China and its five representative cities. On this basis, a surface drainage asphalt pavement combination scheme suitable for rainfall characteristics is proposed. Moreover, the drainage capacity and bearing capacity of the pavement structure are systematically evaluated. The conclusion obtained can provide a reference and guidance for the design of drainage asphalt pavement in North China and similar engineering examples in other regions.

RAINFALL CHARACTERISTICS IN NORTH CHINA AND RAINSTORM INTENSITY INDEX OF REPRESENTATIVE CITIES

General characteristics of rainfall in North China

The temporal and spatial distribution of annual and four-season precipitation in North China has the characteristics of overall consistency. North China is located in the warm temperate zone with a semi-arid and semi-humid monsoon climate, with insufficient but concentrated precipitation, and large regional, seasonal and inter-annual differences. Precipitation decreases from south to north, and the decreasing trend is obvious. The precipitation in the area south of the Yellow River is 700–900 mm, that of the eastern foot of Taihang Mountain and the southern foot of Yanshan Mountain on the western and northern edges of the plain can reach 700–800 mm, the area of Shulu, Nangong and Xianxian in central Hebei province has only 400–500 mm and the Hengshui area in central and southern Hebei province has a rainfall of <500 mm, which is a drought-prone area. Under the background of climate warming, the overall characteristics of precipitation in North China have changed significantly. Precipitation is mainly concentrated in the flood season (May–September), and there are heavy rains. The precipitation in the flood season accounts for about 83.3% of the annual precipitation. According to seasonal statistics, the average precipitation in spring, summer, autumn and winter accounted for approximately. 15.2%, 64.1%, 18.3% and 2.4% of the annual precipitation, respectively. And the inter-annual variation of precipitation is very large, with the relative annual variability reaching 20–30%, and even more than 30% in Beijing, Tianjin and other places (Guo *et al.* 2019a, 2019b).

Taking Beijing as an example, the annual average rainfall is 585 mm, and the rainfall is concentrated in April–September, of which July and August are the main flood season. The rainfall in the multi-year flood season in Beijing accounts for about 72% of the annual rainfall. The sea air mass and the small cold air mass in the north are converging to the south, resulting in a lot of rainfall, and it is mostly

thunderstorms, strong winds and strong convective weather. Every summer, urban waterlogging caused by local heavy rainfall occurs. In recent years, due to the change of climate, the increase of road underlying surface, the rapid development of urban transportation infrastructure, the increase of population and the expansion of the city scale, the rainfall pattern in Beijing has been affected and changed to a certain extent, and the difficulty of urban rainwater treatment has increased (Luo *et al.* 2018a, 2018b; Wang *et al.* 2020).

Rainstorm intensity of representative cities in North China

Rainstorm intensity formula of representative cities in North China

Urban rain pattern characteristics are one of the important references for urban road drainage design. Whether the drainage design matches the urban rain pattern characteristics directly affects the overall planning and future development of a city. Similarly, when carrying out the combined design of urban permeable asphalt pavement structure, systematic analysis of the rain pattern characteristics of Chinese cities can be used not only as the basis for the design of pavement permeability, but also as an evaluation index for comparing and selecting permeable asphalt pavement structures.

At present, the design of the rainstorm intensity formula is the main basis for analyzing the characteristics of the urban rainstorm. This paper selects five representative cities in North China and analyzes the rainstorm intensity for them, which are Beijing, Tianjin, Hohhot, Shijiazhuang and Taiyuan (Shao & Shao 2014; Shao & Liu 2018). The

calculation parameters of the rainstorm intensity formula of each representative city are shown in Table 1.

Analysis of rainstorm intensity in North China representative cities

When researching the characteristics of rainstorm intensity in a certain area, in addition to the design rainstorm return period P and the design rainfall duration t, the design rainstorm type (rain peak position coefficient r) of the area also needs to be considered, and the reference value of the design rainstorm intensity in this area should be determined by comprehensive analysis. In this paper, the Chicago rain pattern generated by the Chicago rain pattern generator is used as the design rain pattern. In the analysis of urban rainstorm characteristics, the pre-concentrated rainfall model is used, which is a short-duration, high-intensity rainfall model, and this rainfall occurs in the early stage of the entire rainfall process. The subsequent research involving the intensity of the rainstorm also uses the Chicago rain pattern generator and combines the design rainstorm intensity formula of representative cities in North China.

In this paper, the rainstorm return period is set to 5 years, the rainfall duration is set to 120 min, and the rain peak position coefficient is set to 0.35. The rainfall characteristics of the five representative cities under this condition obtained by the Chicago rain pattern generator are shown in Figure 1 (Luo *et al.* 2019).

The analysis shows that the total rainfall accumulated in a continuous rainfall event in Beijing, Tianjin, Hohhot, Shijiazhuang and Taiyuan is 67.10 mm, 83.13 mm, 31.76 mm, 61.09 mm and 49.76 mm respectively, and peak rain intensity at 42 min is 3.01 mm/min, 3.23 mm/min, 2.11 mm/min,

Table 1 | Calculation parameters of rainstorm intensity in typical cities

Number	Annual precipitation (mm)	City	Rainstorm intensity formula
1	400–800	Beijing	$i = \dfrac{10.5508(1 + 0.7170\lg P)}{(t + 11.1907)^{0.6867}}$
2	400–800	Tianjin	$i = \dfrac{10.5508(1 + 0.7170\lg P)}{(t + 11.1907)^{0.6867}}$
3	≤400	Hohhot	$i = \dfrac{5.8476(1 + 0.9713\lg P)}{(t + 7.8388)^{0.7464}}$
4	400–800	Shijiazhuang	$i = \dfrac{7.7546(1 + 0.9281\lg P)}{(t + 7.2134)^{0.6666}}$
5	400–800	Taiyuan	$i = \dfrac{11.7502(1 + 1.3319\lg P)}{(t + 19.7773)^{0.8109}}$

Note: *i* is the rainstorm intensity (mm/min); *P* is the design rainstorm return period (a); *t* is the rainfall duration (min).
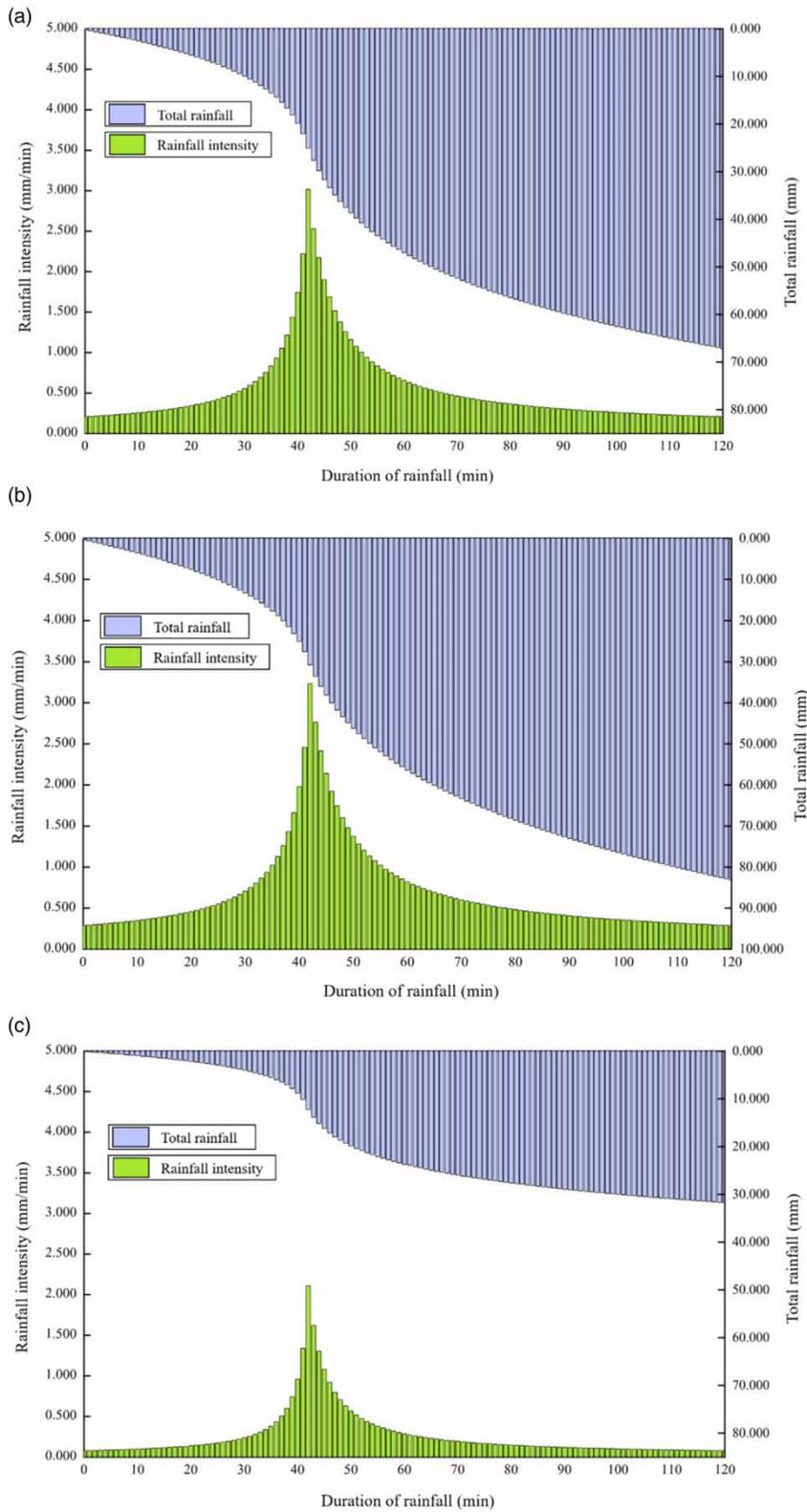
Figure 1 | Rainfall Intensity and total rainfall in representative cities in North China. (a) Beijing. (b) Tianjin. (c) Hohhot. (d) Shijiazhuang. (e) Taiyuan (*continued*).
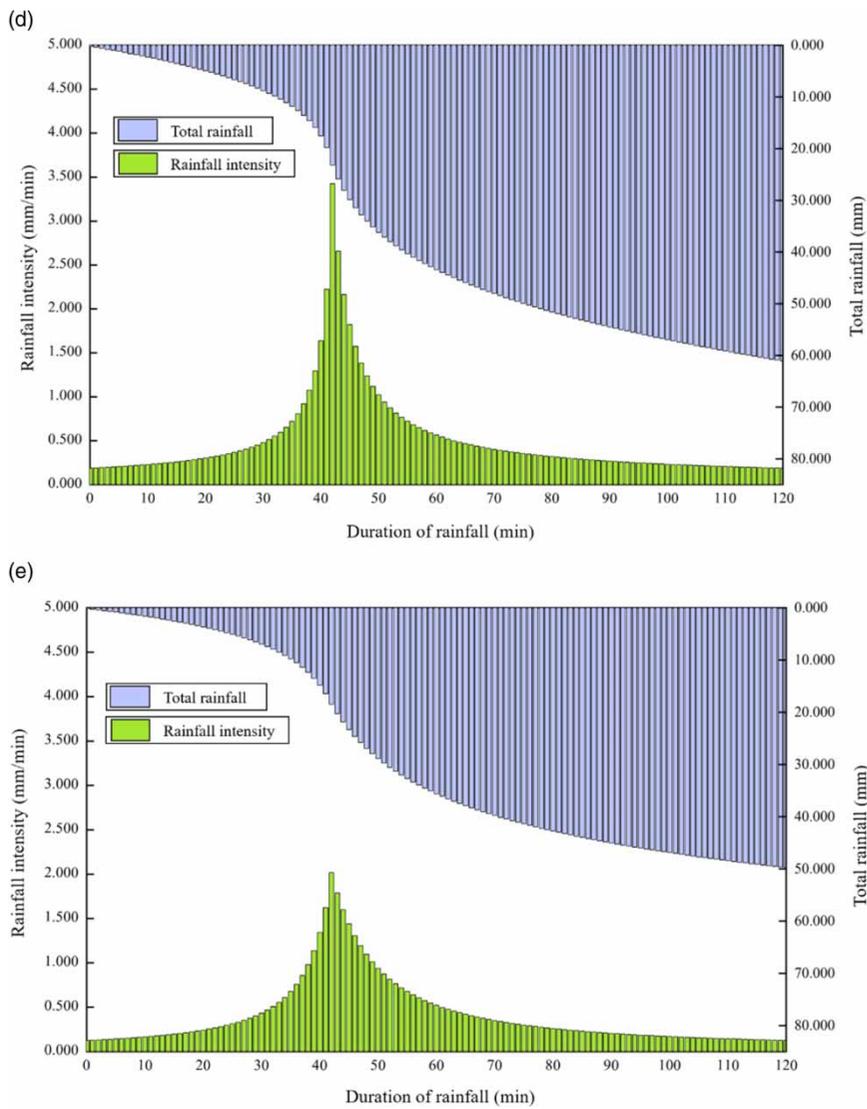
(d)

(e)

Figure 1 | Continued.

3.42 mm/min and 2.01 mm/min respectively. Further calculation shows that the total rainfall accumulated within 30 minutes on both sides of the peak rain intensity is 37.10 mm, 43.17 mm, 19.69 mm, 34.63 mm and 28.68 mm respectively, and the average rain intensity is 0.55 mm/min, 0.69 mm/min, 0.26 mm/min, 0.50 mm/min and 0.41 mm/min respectively.

Rainfall intensity index of representative cities in North China

In order to better analyze the characteristics of the rainstorm near the peak rain intensity, this paper introduces two evaluation indicators, the rain intensity coefficient α and the rainfall index β, to evaluate the change law of the rainfall intensity and the total rainfall during a certain

rainfall period near the peak rain intensity, such as Figure 2 and Formulas (1) and (2).

$$\alpha = \frac{i_t}{i_0} \tag{1}$$

$$\beta = \frac{Q_t}{Q_0} \tag{2}$$

In the formula: i_t is minimum value of rainstorm intensity in the time period t on both sides of the rain intensity peak (mm/min); i_0 is rainstorm intensity peak (mm/min); Q_t is accumulated rainfall in the time period t on both sides of the rain intensity peak (mm); Q_0 is total rainfall during rainfall duration (mm).
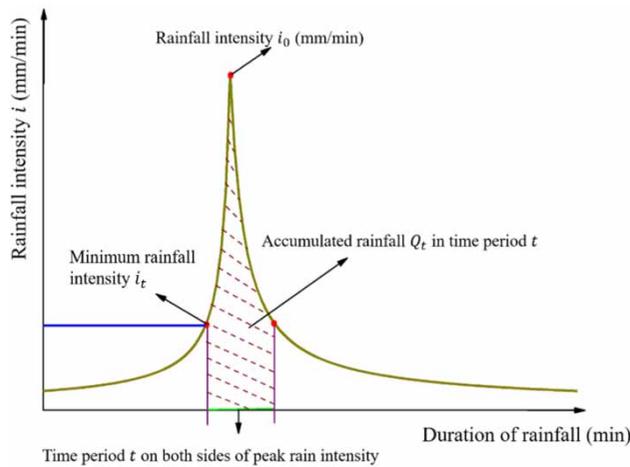
Figure 2 | Schematic diagram of physical meaning of calculation parameters.

The 15 minutes on both sides of the peak rain intensity were selected to further analyze the characteristics of the rainstorm, and the results are shown in Table 2.

It can be seen from Table 2 that among the five representative cities, the rain intensity coefficient of Hohhot is relatively small and the rainfall index is relatively high, while the rain intensity coefficients of the other four cities are between 0.32 and 0.43, and the rainfall index is between 0.34 and 0.41. It can be considered that Beijing, Tianjin, Shijiazhuang and Taiyuan have the same rainfall characteristics, which are more typical and representative than Hohhot.

Analysis of urban rainfall seepage and drainage process in North China

There are two situations in the urban rainfall seepage and drainage process in North China according to whether the soil foundation is permeable: when the soil foundation is permeable, the seepage and drainage process is road surface soaking → infiltration → complete   infiltration → drainage (drainage   pipe   drainage + continued   infiltration) → road

surface accumulation (excessive rain intensity) → stop rain drainage (drainage pipe drainage + continued infiltration) → drying; when the soil foundation is impervious, the seepage and drainage process is road surface soaking → infiltration → complete   infiltration → drainage   (drainage pipe drainage) → road surface accumulation (excessive rain intensity) → stop rain drainage (drainage pipe drainage) → dry. The rain seepage and drainage process of permeable soil foundation and impervious soil foundation are shown in Figures 3 and 4.

ANALYSIS OF SPONGE ROAD DRAINAGE PAVEMENT STRUCTURE ADAPTED TO THE CHARACTERISTICS OF RAINSTORM IN NORTH CHINA

Scheme comparison and structural combination of sponge road drainage pavement

Drainage asphalt pavement structure mainly includes three parts: surface layer, base layer and subgrade, which are divided into three typical structural types: surface layer drainage, pavement drainage and permeable road. Among them, surface layer drainage is divided into single surface layer drainage and double surface layer drainage. The surface layer of surface layer drainage asphalt pavement is permeable and draining, and the pavement bearing capacity is relatively good. It is generally suitable for urban environments with heavy traffic volume and low rainfall intensity. Pavement drainage asphalt pavement is permeable to rain at the surface layer and base layer, and has a drainage pipe at the base layer, and also has a good road bearing capacity. It is generally suitable for urban environments with moderate traffic volume and moderate rainfall intensity. Permeable road asphalt pavement surface layer, base layer, subbase layer and subgrade are all permeable, and the subgrade drainage pipe drains rain. Permeable road asphalt pavement is generally suitable for

Table 2 | Calculation results of rainstorm characteristics in Beijing

Characteristic index	Peak rain intensity i_0	Total rainfall Q_0	Rain intensity minimum i_{15}	Accumulated rainfall Q_{15}	Rain intensity coefficient α_{15}	Rainfall index β_{15}
Beijing	3.0162	67.1031	1.0247	25.4119	0.3397	0.3787
Tianjin	3.2302	83.1308	1.2304	28.6873	0.3809	0.3451
Hohhot	1.8112	31.7571	0.4912	14.5720	0.2712	0.4589
Shijiazhuang	3.0251	61.0896	0.9842	24.8534	0.3253	0.4068
Taiyuan	2.0172	49.7608	0.8652	20.1674	0.4289	0.3852

(a) Road surface soaking

(b) Rain seeps

(c) Seepage and drainage of permeable soil base

(d) Road surface accumulation

(e) Stop drain

(f) Emptying of accumulated water
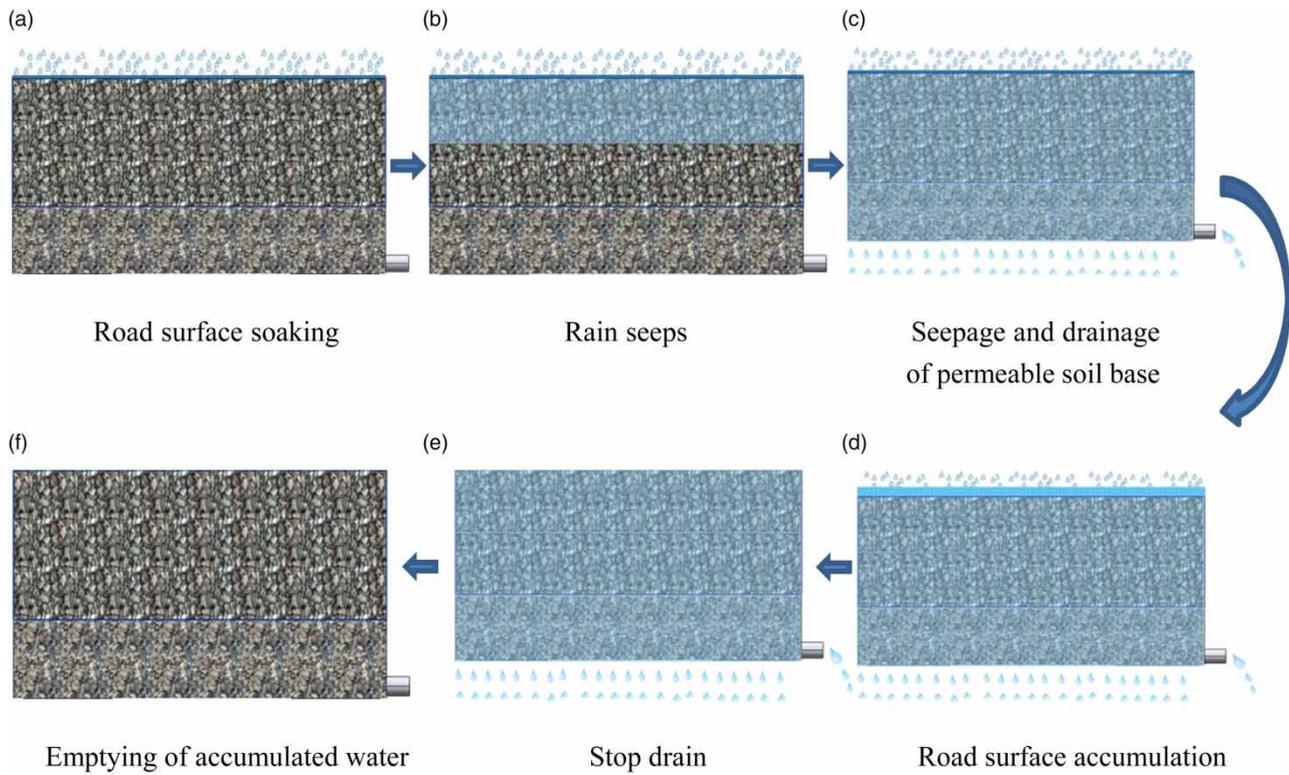
Figure 3 │ Rainfall seepage and drainage process of permeable soil base.

(a) Road surface soaking

(b) Rain seeps

(c) Drainage of impervious soil base

(d) Road surface accumulation

(e) Stop drain

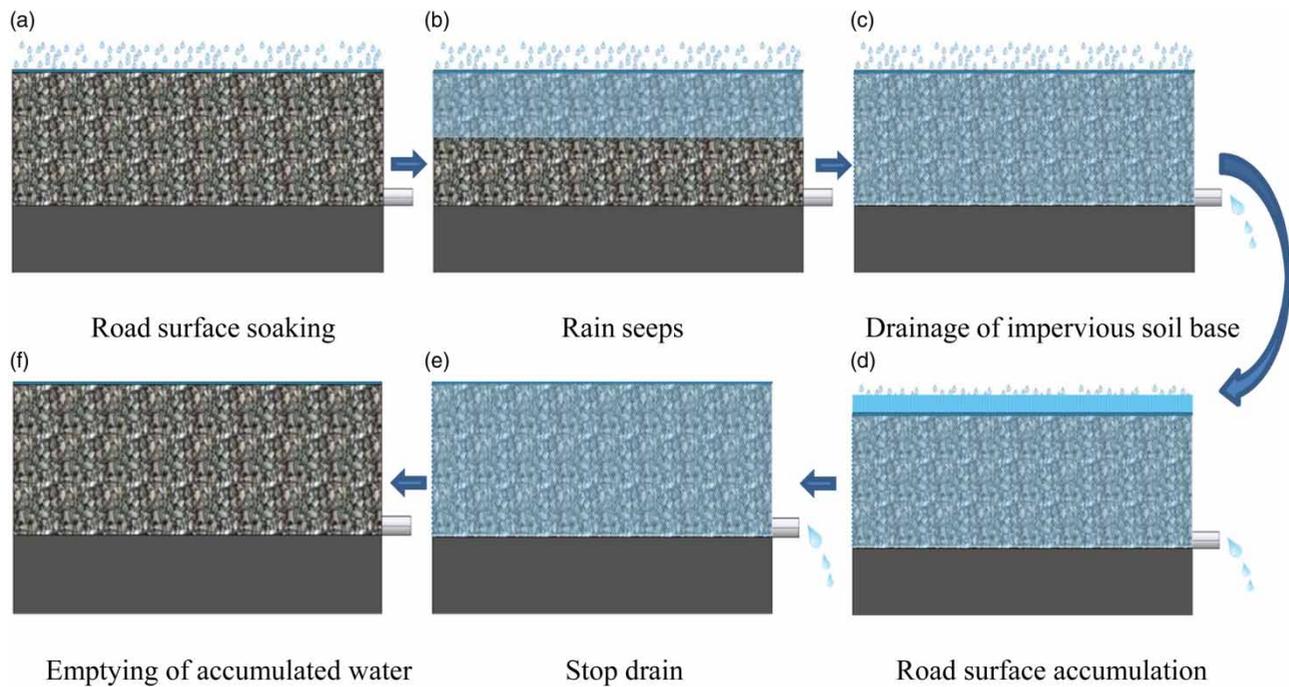(f) Emptying of accumulated water

Figure 4 │ Rainfall seepage and drainage process of impervious soil base.

urban environments with small traffic volume and high rainfall intensity (Wang *et al.* 2019).

Considering the characteristics of sudden rainfall, high rainfall, short duration, and large inter-annual variability in Beijing, and that its traffic volume, especially in the downtown area, is huge and the drainage capacity of the surface drainage pavement structure is limited, it is difficult to solve the flood disasters in Beijing during the flood season, especially in the downtown area. Furthermore, the permeable road pavement structure has more permeable layers, and cannot meet the road bearing capacity requirements of Beijing's downtown. Therefore, this paper intends to adopt the drainage pavement structure in Beijing.

In the pavement drainage asphalt pavement structure of the road surface, not only is the surface layer a permeable structure, but also part of the base layer is also set as a permeable structure, so the thickness of the permeable layer is large, meaning this structure can be applied to the urban environment with high rainfall intensity and large traffic volume. Because it is thicker than the surface drainage type, the default surface layer in this study is double drainage layer structure. Also, the upper base layer is set as a drainage structure in this paper; at the same time, a modified emulsified asphalt seal layer is set between the upper base layer and the subbase, which means the rainwater infiltrated into the pavement upper base layer will not continue to seep into the subbase, and can only be discharged along the bottom of the upper base layer. The design of pavement drainage asphalt pavement studied in this paper is a combination of double drainage surface layer and permeable base layer, and the typical structure of pavement drainage asphalt pavement is shown in Figure 5.
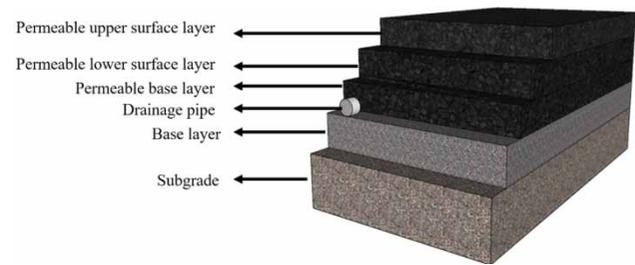

Figure 5 | Typical structure of drainage asphalt pavement.

Design method and parameter determination of pavement permeability function

Because only the connected pores have a permeation effect in the permeable pavement, the void ratio in the permeable pavement is calculated based on the connected porosity. In this paper, the permeable porous structure is equivalent to the structure of an aquifer and connected pore structure, as shown in Figure 6.

Under a continuous rainfall event, the thickness of the permeable pavement structure layer is changed to obtain data such as the time of surface runoff on the permeable asphalt pavement, the total amount of surface runoff, and the maximum water storage height of the pavement permeable layer. By establishing the functional relationship between the thickness of the pavement permeable structure layer and the total surface runoff, the recommended design thickness of the permeable structure layer, when the permeable asphalt pavement has no surface runoff under the continuous rainfall event, is calculated. The equivalent water storage depth of surface layer and the void ratio of permeable structure layer are calculated as
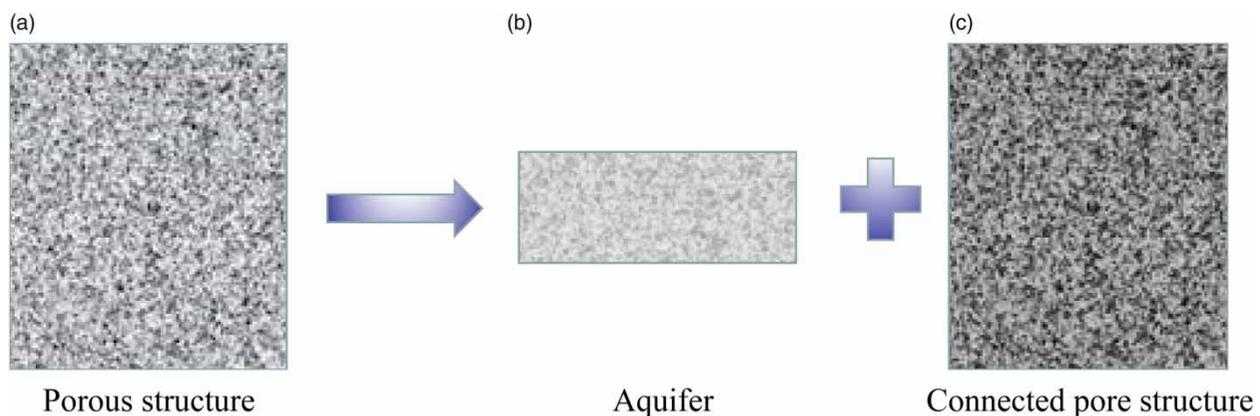

Figure 6 | Equivalent calculation model of surface layer water storage depth.

shown in Formula (3).

$$h = a^*H \tag{3}$$

In the formula: h is equivalent water storage depth of the surface layer (mm); a is water adhesion rate (%); for porous asphalt material, when the porosity is 20%, a is 1.5; for graded gravel material, when the porosity is 10%, a is 0.5; H is thickness of porous material (mm).

In addition, in this paper, the porosity of the permeable surface layer and the permeable base layer material are both set to 20%; then referring to the relevant literature, the connected porosity vv' and the permeability coefficient k can be calculated by Formulas (4) and (5) (Jiang 2011; Jiang et al. 2015; Yang et al. 2019):

$$vv' = 0.6888vv + 1.8955 \tag{4}$$

$$k = 5.59vv' - 0.2887 \tag{5}$$

vv' is connected porosity of permeable structural layer (%)
vv is porosity of permeable structural layer (%).

Calculation with Formula (4) shows that the connected porosity of the permeable structure layer is 15.67%; with Formula (5), the corresponding permeability coefficient k

is 0.59 cm/s (that is, 354 mm/min); calculation with Formula (3) shows that the equivalent water storage depth (h) of the surface layer under different permeable layer thickness (H) is 0.015H, and the specific parameter settings are shown in Table 3.

Analysis method and parameter determination of pavement structure bearing capacity

In this paper, BISAR3.0 software is used to analyze the structure of permeable asphalt pavement. The loading method mainly refers to the 'Highway Asphalt Pavement Design Specification' (JTG D50-2017 2017). the loading method mainly refers to specifications for design of highway asphalt pavement (JTG D50-2017 2017), and the elastic layered system theory under the action of double circular vertical uniform load is used to calculate and analyze permeable asphalt pavement. The standard axle load is 100 kN, the tire pressure is 0.7 MPa, the load radius is 106.5 mm, the center distance between two wheels is 319.5 mm, and the state analysis model of completely continuous interlayer contact is used to calculate A (unit load center), B (tire inside edge), C (center of wheel spacing) and D (midpoint of B–C) respectively (JTG D50-2017 2017). The calculation model is shown in Figure 7.

Through the permanent deformation of the asphalt mixture layer and the vertical compressive strain of the top

Table 3 | Main setting parameters of pavement drainage asphalt pavement

| Surface layer	Ranges	Permeable pavement layer	Ranges	Bottom drainage layer	Ranges
Equivalent water storage depth (mm)	0.015H	Thickness (mm)	H	Drainage coefficient (mm/h)	0
Vegetation coverage coefficient	0	Permeability coefficient	0.59	Drainage index	0
Surface roughness coefficient	0.013	Impervious coefficient	0	Offset height of culvert (mm)	0
Surface slope	2.0	Permeability (mm/h)	15,480		
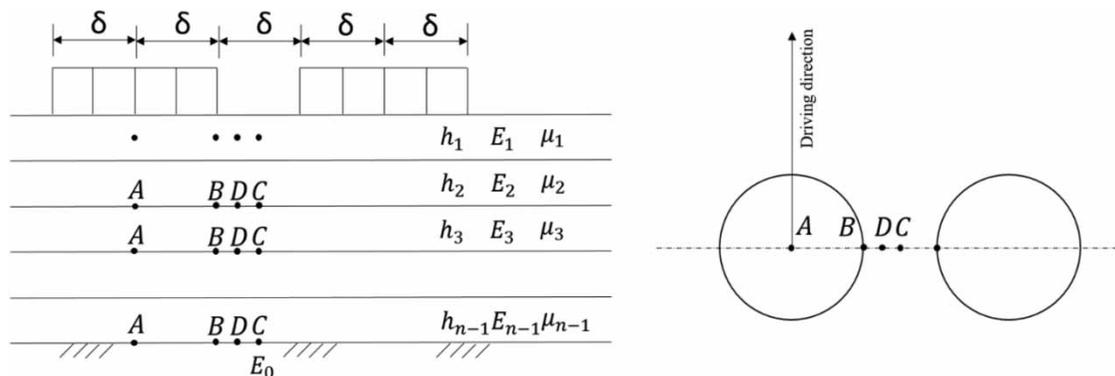
Figure 7 | Calculation scheme of control index value for permeable asphalt pavement.

surface of the subgrade, the thickness combination conforms to the bearing capacity of the Beijing permeable road. The Formulas (6), (7), (8) and (9) calculate the permissible permanent deformation of the asphalt mixture layer as follows:

$$R_a = \sum_{i=1}^{n} R_{ai} \tag{6}$$

$$R_{ai} = 2.31*10^{-8}k_{Ri}T_{pef}^{2.93}p_i^{1.80}N_{e3}^{0.48}(h_i/h_0)\,R_{0i}$$

$$k_{Ri} = (d_1 + d_2 * z_i) * 0.9731^{zi} \tag{7}$$

$$d_1 = -1.35 * 10^{-4}h_a^2 + 8.18 * 10^{-2}h_a - 14.50 \tag{8}$$

$$d_2 = 8.78 * 10^{-7}h_a^2 - 1.50 * 10^{-3}h_a + 0.90 \tag{9}$$

R_a is permissible permanent deformation of asphalt mixture layer (mm)

R_{ai} is permanent deformation of the i-th layer (mm)

n is number of layers

T_{pef} is permanent deformation equivalent temperature of asphalt mixture layer (°C)

N_{e3} is cumulative number of times of equivalent design axle load on the design lane within the design service life or the opening to traffic to the first repair period for rutting

h_i is thickness of the i layer (mm)

h_0 is thickness of rutting test specimen (mm)

R_{0i} is permanent deformation of the rutting test, when the test temperature of the i-th layered asphalt mixture is 60 °C, the pressure is 0.7 MPa, and the number of loading times is 2,520

p_i is vertical compressive stress of the top surface of the i-th layer of asphalt mixture (MP)

k_{Ri} is comprehensive correction factor

z_i is depth of the i-th layer of the asphalt mixture layer (mm); the first layer is taken as 15 mm, and the other layers are the depth from the road surface to the midpoint of the layer

h_a is asphalt mixture layer thickness (mm); when h_a is larger than 200 mm, take 200 mm.

The values of each parameter can be directly obtained or calculated by referring to *Specifications for Design of Highway Asphalt Pavement* (JTG D50-2017 2017), in which h_a can be adjusted according to Table 6 to calculate d_1 and d_2, and z_i can also be adjusted according to Table 6 to calculate k_{Ri}; combined with the characteristics of annual/monthly average temperature changes in Beijing, T_{pef} is calculated to be 20.18 °C; p_i can be calculated with BISAR3.0; within the set service life, N_{e3} is set to 9 million times; h_i is listed in Table 6; h_0 is 50 mm; in this paper, the permeable road

asphalt mixture has the same upper and lower layer materials. Through the rutting test, it is determined that R_{0i} is 5.788 mm; after determining all of the required parameters, the value of R_a can be calculated by summing (JTG D50-2017 2017).

Formula (10) calculates the permissible vertical compressive strain on the top surface of subgrade as follows:

$$[\varepsilon_z] = 1.25*10^{4-0.1\beta}(k_{T3}N_{e4})^{-0.21} \tag{10}$$

ε_z is permissible vertical compressive strain of subgrade top surface (10^{-6})

β is target reliability index, which depends on the grade of the roads: take 1.65 for expressways, 1.28 for first-class roads, 1.04 for second-class roads, 0.84 for third-class roads and 0.52 for fourth-class roads

N_{e4} is cumulative number of equivalent design axle loads on the design lane within the design service life

k_{T3} is temperature adjustment factor.

Refer to *Specifications for Design of Highway Asphalt Pavement* (JTG D50-2017 2017) to directly obtain or calculate the value of each parameter: β adopts the first-level kilometer index to be 1.28; N_{e4} is the same as N_{e3}, take 9 million times; k_{T3} is calculated as 1.088 through the specification; then ε_z can be calculated (JTG D50-2017 2017).

Refer to *Permeable Asphalt Pavement Technical Specification* (CJJ/T 190-2012) to determine the pavement structure materials and their performance parameters as shown in Table 4 (Ding *et al.* 2019).

Results analysis and discussion

Results analysis of pavement permeability design

According to the characteristics of urban rainstorm in Beijing, this paper sets the total thickness of permeable

Table 4 | Main material parameters of pavement structural layers

Structural layer material	Compressive modulus at 20 °C/MPa	Poisson's ratio	Structure layer thickness/mm
PAC-13(20)	700	0.25	—
ATPB-25	800	0.25	—
Inorganic binder stabilized gravel	1,500	0.25	150
Inorganic binder stabilized soil	800	0.25	300
Subgrade cohesive soil	40	0.35	—

structural layers to be 90 mm, 100 mm, 110, 120 and 130 mm respectively, and calculates the total runoff on asphalt pavement and the water storage height inside the pavement structure under different thickness of permeable structural layers by using rainstorm runoff simulation software SWMM5.1. The specific calculation results are shown in Table 5 and Figure 8.

Combining Table 5 and Figure 8, it can be seen that as the total thickness of the permeable structure layer increases, the total road surface runoff and the start time of road surface runoff gradually decrease, and the maximum water storage height in the pavement structure gradually increases. This shows that increasing the thickness of the permeable structure layer can effectively reduce the total amount of road surface runoff and delay the appearance of road surface runoff. This is because, on the one hand, the increase in the thickness of the permeable structure layer can make it absorb more rainwater. On the other hand, the increase in the thickness of the permeable structure layer can also accumulate more rainwater in its connected pores, delaying the appearance of road surface runoff; at the same time, due to the thickness of permeable structure layer increases, the buried depth of drainage pipe laid at its bottom will increase, and the water head height of drainage pipe will increase when collecting and discharging rainwater, thereby improving its ability to discharge rainwater infiltrated into the pavement structure.

Combining Table 5 and Figure 8, it can also be seen that by changing the total design thickness of the permeable structure layer, the surface runoff of urban roads can be avoided in a rainstorm. Therefore, in this section, through the data fitting analysis of the total thickness of the permeable structure layer and the total road surface runoff in Table 5, with the help of the numerical fitting results analysis of the two, it is possible to obtain the total design thickness of the permeable structural layer that meets the characteristics of the rainstorm in Beijing and avoids road surface runoff, and the specific analysis results are shown in Figure 9.

It can be seen from Figure 9 that for the characteristics of urban rainstorm in Beijing, this paper calculates that there is a negative correlation between the total design thickness of the permeable structure layer and the total road surface runoff. By further fitting the numerical relationship between them, it can be concluded that the relationship formula is shown in Formula (11)

$$Q = 88.12e^{-H/116.81} - 21.22 \qquad (11)$$
$$R^2 = 0.9237 \qquad (12)$$

It can be calculated from Formula (11) that when there is no road surface runoff, the total design thickness of the permeable layer is 166.31 mm, that is, the total design thickness of the permeable structure layer that meets the characteristics of the rainstorm in Beijing and has no road surface runoff can be 170 mm.

Results analysis of pavement bearing capacity design

Based on the selection of the materials of each structural layer of the permeable asphalt pavement and the determination of the parameters, this section uses BISAR3.0 to analyze the surface deflection of the drainage asphalt pavement, the maximum tensile stress at the bottom of asphalt surface layer and the maximum tensile stress at the bottom of semi-rigid base layer with different thickness combination of road surface permeable structure layer, and the calculation results are shown in Table 6.

It can be seen from Table 6 that for the nine combinations of permeable pavement asphalt pavements designed, the maximum values of the vertical compressive strain on the top surface of the subgrade and the permanent deformation of the asphalt mixture layer are less than the minimum value in the specification. When the thickness of permeable surface layer is the same, with the increase of the thickness of permeable base layer, the compressive strain on the top of subgrade and the permanent deformation of asphalt mixture

Table 5 | Simulation results under different permeable layer thickness

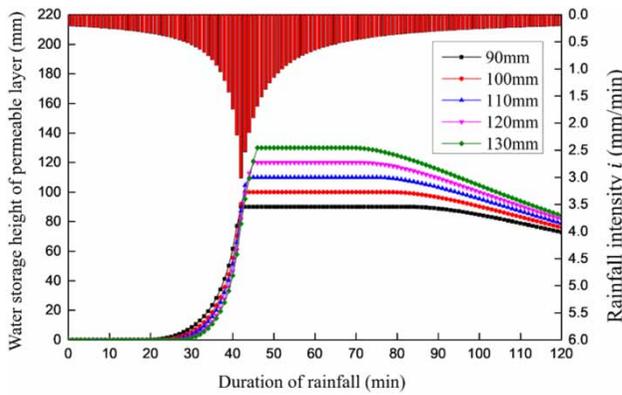| No.	Thickness of permeable surface H/mm	Total rainfall Q_0/mm	Total road surface runoff Q/mm	Pavement drainage-seepage ratio γ/%	Start time of road surface runoff t/min	Maximum water storage height of pavement structure H_0/mm
1	90	66.8957	19.6804	29.42	42	90
2	100	66.8957	16.0903	24.05	43	100
3	110	66.8957	13.2516	19.81	44	110
4	120	66.8957	10.1325	15.14	45	120
5	130	66.8957	7.8347	11.71	46	130

Figure 8 │ Calculation results of surface runoff under different permeable layer thickness.
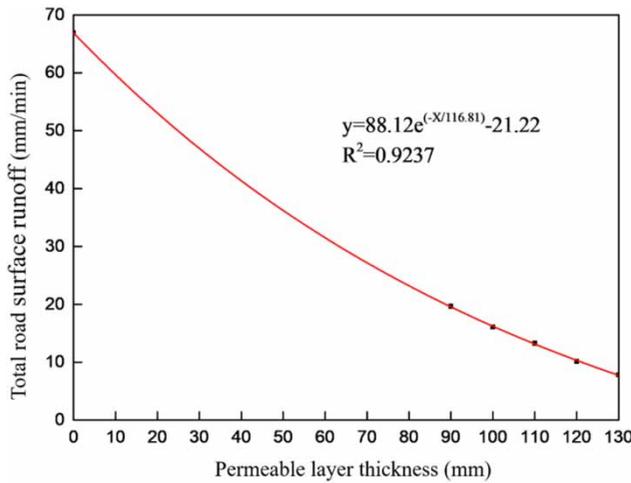

Figure 9 │ Fitting analysis of total design thickness of permeable layer and total road surface runoff.

layer will decrease; when the thickness of permeable base is the same, with the increase of the thickness of permeable surface layer, the compressive strain on the top of subgrade and the permanent deformation of asphalt mixture layer also decrease. This indicates that optimizing the thickness of the permeable structure layer can effectively improve the overall bearing capacity of the pavement. At the same time, increasing the thickness of permeable structure layer can also improve the bearing capacity of pavement drainage asphalt pavement.

Comprehensive analysis shows that the pavement drainage asphalt pavement structure can further improve the permeability and drainage capacity of asphalt pavement by changing some or all impervious base layers of pavement drainage asphalt pavement into permeable macroporous asphalt stabilized macadam base layers, thereby avoiding the problem of urban waterlogging in Beijing during heavy rain. At the same time, since the base layer of this pavement structure is flexible with a porous structure, its bearing capacity is smaller than that of the surface drainage asphalt pavement, but it can still meet the design requirements of the medium traffic level urban road bearing capacity.

CONCLUSIONS

Based on the research and analysis of the characteristics of urban rainstorm patterns in Beijing, a representative city in northern China, this paper suggests that pavement drainage asphalt pavement should be used to solve the problem of urban road rainwater infiltration and drainage in rainstorm

Table 6 │ Main indexes of asphalt pavement with different permeable layer thickness

No.	Thickness of permeable structure layer H/mm		Vertical permissible compressive strain on the top surface of subgrade ε_z	Vertical calculation of compressive strain on the top surface of subgrade ε_z	Permissible permanent deformation of asphalt mixture layer R_a/0.1 mm	Cumulative permanent deformation of asphalt mixture layer R_a/0.1 mm
	Surface layer	Base layer				
1	40 + 50	80	316.80	312.20	10.57	10.17
2	40 + 50	90	316.80	303.80	10.57	9.72
3	40 + 50	100	316.80	295.80	10.57	9.63
4	50 + 50	80	316.80	304.20	12.74	10.02
5	50 + 50	90	316.80	296.20	12.74	9.70
6	50 + 50	100	316.80	288.40	12.74	9.59
7	50 + 60	70	316.80	304.60	12.64	10.05
8	50 + 60	80	316.80	296.50	12.64	9.96
9	50 + 70	80	316.80	289.10	12.46	9.90

days. On this basis, the rainstorm runoff simulation software SWMM5.1 and the pavement structure analysis software BISAR3.0 are used to calculate and analyze the pervious functions and bearing capacity of the surface drainage asphalt pavement. The main conclusions are as follows.

(1) In view of the rainstorm recurrence period of 5 years, rainfall duration of 120 min and rainfall peak location coefficient of 0.35, it is calculated that the total amount of rainfall accumulated in a continuous rainfall event in Beijing is 66.8975 mm, and the peak of rainfall intensity at 42 min is 3.0162 mm/min.

(2) In view of the urban rainstorm characteristics of Beijing, the rainwater seepage and drainage of urban roads is simulated and analyzed by using SWMM5.1 software. Through calculation, the minimum total design thickness of the permeable surface layer and permeable base layer that meets the road drainage requirements in the area is 170 mm.

(3) With the help of BIASR3.0 software, the pavement structure of permeable asphalt pavement with different permeable surface thickness is analyzed. The results indicate that the permanent deformation of asphalt mixture layer and vertical compressive strain of subgrade top surface of the nine pavement structure combinations designed in this paper meet the requirements of the specifications, and can be used for the structural design of permeable pavement in Beijing.

DATA AVAILABILITY STATEMENT

All relevant data are included in the paper or its Supplementary Information.

REFERENCES

Afonso, M., Fael, C. & Dinis-Almeida, M. 2017 Permeable asphalt pavement as a measure of urban green infrastructure in the extreme events mitigation. *World Academy of Science, Engineering and Technology* **11** (10), 1455.

Bean, E., Clark, M. & Larson, B. 2019 Permeable pavement systems: technical considerations. *EDIS* **2**. Retrieved from: https://journals.flvc.org/edis/article/view/106902.

Ding, X. H., Ma, T. & Huang, X. M. 2019 Discrete-element contour-filling modeling method for micro- and macro-mechanical analysis of aggregate skeleton of asphalt mixtfre. *Journal of Transportation Engineering, Part B: Pavements* **145** (1). doi:10.1061/jpeodx.0000083.

Guo, J., Xiong, M. M. & Huang, H. 2019a Analysis of diurnal variation characteristics of rainfall during warm season in Beijing-Tianjin-Hebei region. *Johnal of Marine Metrology* **39** (2), 58–67. doi:10.19513/j.cnki.issn2096-3599.201.92.006 (in Chinese).

Guo, L., Sun, M. L., Wang, X. J. & Lan, H. 2019b Statistical analysis of the characteristics difference of rainfall over Bohai Bay and the land. *Climate Change Research Letters* 835–844. https://doi.org/10.12677/CCRL.2019.86092 (in Chinese).

Heweidak, M. & Amin, S. 2019 Effects of OASIS phenolic foam on hydraulic behaviour of permeable pavement systems. *Journal of Environmental Management* **230**, 212–220.

Jiang, W. 2011 *Composition Design and Function Evaluation for Materials and Structure of Permable Asphalt Pavement*. Chang'an University, Xi'an, China.

Jiang, W., Sha, A. M. & Xiao, J. J. 2015 Experimental study on relationships among composition, microscopic void features, and performance of porous asphalt concrete. *Journal of Materials in Civil Engineering* **27** (11). doi:10.1061/(asce)mt.1943-5533.0001281.

JTG D50-2017 2017 *Specifications for Design of Highway Asphalt Pavement*. China Road and Bridge Technology Co., Ltd, Beijing, China.

Kia, A., Wong, H. S. & Cheeseman, C. 2019 High-strength clogging resistant permeable pavement. *International Journal of Pavement Engineering*. doi.org/10.1080/10298436.2019.1600693.

Liu, Y., Li, T. & Peng, H. Y. 2018 A new structure of permeable pavement for mitigating urban heat island. *Science of The Total Environment* **634**, 1119–1125.

Luo, M. 2017 Mechanical analysis of asphalt stabilized permeable base to inhibit reflective cracking. *Materials Science and Engineering Conference Series* **231**, 012090.

Luo, P. P., Mu, D. R., Xue, H., Ngo-Duc, T., Dang-Dinh, K., Takara, K., Nover, D. & Schladow, G. 2018a Flood inundation assessment for the Hanoi Central Area. Vietnam Under Historical and Extreme Rainfall Conditions. *Scientific Reports* **8**, 12623.

Luo, P. P., Zhou, M. M., Deng, H. Z., Lyu, J. Q., Cao, W. Q., Takara, K., Nover, D. & Geoffrey Schladow, S. 2018b Impact of forest maintenance on water shortages: hydrologic modeling and effects of climate change. *Science of the Total Environment* **615**, 1355–1363.

Luo, P. P., Kang, S. X., Apip, Zhou, M. M., Lyu, J. Q., Aisyah, S., Regmi, R. K. & Nover, D. 2019 Water quality trend assessment in Jakarta: a rapidly growing Asian megacity. *PLoS ONE* **14**, e0219009. doi: 10.1371/journal.pone.0219009.

Manikanta, V. & Reddy, G. 2018 Construction of permeable asphalt pavement using recron fiber. *International Journal of Engineering Technology Science and Research* 5 (1), 1124–1127.

Masoud, K., Li, H., John, T. H. & Liang, X. 2019 Application of permeable pavements in highways for stormwater runoff management and pollution prevention: California research experiences. *International Journal of Transportation Science and Technology* 12, 358–372.

Shao, D. N. & Liu, S. G. 2018 Up-to-date urban rainstorm intensity formulas considering spatial diversity in China. *Environmental Earth Sciences* 77 (14), 541.

Shao, Y. M. & Shao, D. N. 2014 *Chinese New Generation of Rainstorm Intensity Formula*. Chinese Architecture & Buildinig Press, p. 11. https://doi.org/10.13789/j.cnki.wwe1964.2014.0358.

Sun, Y. Z., Guo, R., Wang, X. C. & Ning, X. H. 2019 Dynamic response characteristics of permeable asphalt pavement based on unsaturated seepage. *International Journal of Transportation Science and Technology* 8, 403–417.

Tziampou, N., Coupe, S., Sañudo-Fontaneda, L., Newman, A. & Castro-Fresno, D. 2020 Fluid transport within permeable pavement systems: a review of evaporation processes, moisture loss measurement and the current state of knowledge. *Construction & Building Materials* 243, 118179.

Wang, H., Li, H., Liang, X., Zhou, H., Xie, N. & Dai, Z. 2019 Investigation on the mechanical properties and environmental impacts of pervious concrete containing fly ash based on the cement-aggregate ratio. *Construction and Building Materials* 202, 387–395. doi:10.1016/j.conbuildmat.2019.01.044.

Wang, Y. C., Gao, Q., Du, L. G., Ma, J. W. & Liu, Y. F. 2020 Analysis of precipitation characteristics during the flood seasons in Beijing. *China Flood & Drought Management* 30 (2). doi:10.16867/j.issn.1673-9264.2018254.

Wendling, L. & Holt, E. 2019 Integrating engineered and nature-based solutions for urban stormwater management. *Women in Water Quality: Investigations by Prominent Female Engineers* 23–46. doi:10.1007/978-3-030-17819-2_2.

Yang, B., Li, H., Zhang, H. J., Xie, N. & Zhou, H. 2019 Laboratorial investigation on effects of microscopic void characteristics on properties of porous asphalt mixture. *Construction and Building Materials.* 213, 434–446.

Yin, J. M., Miao, S. L., Li, S. Q. & Meng, W. 2018 Material design and performance analysis of porous cement stabilized macadam. *IOP Conference Series: Earth and Environmental Science* 186, 012015.